

Article

# Mitigating the Effects of Climate Change through Harvesting and Planting in Boreal Forests of Northeastern China

Xu Luo <sup>1,\*</sup>, Hong S. He <sup>2</sup>, Yu Liang <sup>3</sup>, Jacob S. Fraser <sup>2</sup> and Jialin Li <sup>1</sup>

<sup>1</sup> Department of Geography & Spatial Information Techniques, Ningbo University, Ningbo 315211, China; nbnj2001@163.com

<sup>2</sup> School of Natural Resources, University of Missouri, Columbia, MO 65211, USA; heh@missouri.edu (H.S.H.); fraserjs@missouri.edu (J.S.F.)

<sup>3</sup> Institute of Applied Ecology, Chinese Academy of Science, Shenyang 110016, China; liangyu@iae.ac.cn

\* Correspondence: luoxu99@hotmail.com; Tel.: +86-574-8760-2769

Received: 11 July 2018; Accepted: 26 September 2018; Published: 1 October 2018



**Abstract:** The ecological resilience of boreal forests is an important element of measuring forest ecosystem capacity recovered from a disturbance, and is sensitive to broad-scale factors (e.g., climate change, fire disturbance and human related impacts). Therefore, quantifying the effects of these factors is increasingly important for forest ecosystem management. In this study, we investigated the impacts of climate change, climate-induced fire regimes, and forest management schemes on forest ecological resilience using a forest landscape model in the boreal forests of the Great Xing'an Mountains, Northeastern China. First, we simulated the effects of the three studied variables on forest aboveground biomass, growing space occupied, age cohort structure, and the proportion of mid and late-seral species indicators by using the LANDIS PRO model. Second, we calculated ecological resilience based on these four selected indicators. We designed five simulated scenarios: Current fire only scenario, increased fire occurrence only scenario, climate change only scenario, climate-induced fire regime scenario, and climate-fire-management scenario. We analyzed ecological resilience over the five scenarios from 2000 to 2300. The results indicated that the initialized stand density and basal area information from the year 2000 adequately represented the real forest landscape of that year, and no significant difference was found between the simulated landscape of year 2010 and the forest inventory data of that year at the landscape scale. The simulated fire disturbance results were consistent with field inventory data in burned areas. Compared to the current fire regime scenario, forests where fire occurrence increased by 30% had an increase in ecological resilience of 12.4–43.2% at the landscape scale, whereas increasing fire occurrence by 200% would decrease the ecological resilience by 2.5–34.3% in all simulated periods. Under the low climate-induced fire regime scenario, the ecological resilience was 12.3–26.7% higher than that in the reference scenario across all simulated periods. Under the high climate-induced fire regime scenario, the ecological resilience decreased significantly by 30.3% and 53.1% in the short- and medium-terms at landscape scale, while increasing slightly by 3.8% in the long-term period compared to the reference scenario. Compared to no forest management scenario, ecological resilience was decreased by 5.8–32.4% under all harvesting and planting strategies for the low climate-induced fire regime scenario, and only the medium and high planting intensity scenarios visibly increased the ecological resilience (1.7–15.8%) under the high climate-induced fire regime scenario at the landscape scale. Results from our research provided insight into the future forest management and have implications for improving boreal forest sustainability.

**Keywords:** Ecological resilience; fire disturbance; forest landscape; The Great Xing'an Mountains; LANDIS

## 1. Introduction

Boreal forests are the northern-most forested biomes, and are expected to be sensitive to climate change and forest fire disturbances [1]. By 2100, the climate in Northern high latitudes (including North America and Eurasia) is expected to increase by 1.4 to 5.8 °C, about 5 times greater than the global mean temperature increase [2,3]. Recent studies have projected that climate change will affect the species distribution and ecosystem functions (e.g., carbon fixation) within boreal forests [4]. For instance, climate change can alter interspecific competition and tree species migration [5], which could further affect forest composition and distribution [6]. Species response to climate change varied among and within populations of different trees in the boreal forests [7]. Changes in climatic conditions (e.g., precipitation and temperature) can have direct influences on the metabolic processes, growth rates, establishment abilities, and competitive ability of trees, thus affecting overall biomass accumulation in forests [5,8]. These resulting changes in forest structure and function are expected to affect the recovery ability (ecological resilience) of boreal forests at landscape scales [9]. Additionally, climate change indirectly impacts forest traits (e.g., forest structure, composition, and ecological resilience) through its effects on fires regimes [10]. In boreal forests, climate-induced fires are frequent and widespread, and become a major factor that can distinctly affect forest successional dynamics, composition, and structure [11,12]. Johnstone et al. [11] showed that forest fires with increased severity may promote shifts from coniferous forest to deciduous-dominated forests, and substantially change landscape dynamics and ecosystem services in boreal forests. More previous studies indicated that fires have been projected to occur more frequently, burn greater areas, and have higher intensities under altered climatic conditions [13,14]. As a result of climate change altered fire regimes, forest composition and biomass dynamics, and thus ecological resilience is expected to shift [15]. Despite the growing evidence that climate change and shifting fire regimes will alter the composition, structure and biomass of boreal forests, quantification of how these two factors will impact forest ecological resilience is still poorly known.

Ecological resilience is characterized as the capacity of a forest ecosystem to recover from disturbance and maintain a stable state, supporting the recovery of structure, composition, and function equivalent to pre-disturbance states [16]. Boreal forests were remarkably resilient to disturbances, and forest species were adapted to the current disturbance regimes with long term effects [17]. For the existence of forest ecological resilience, boreal forest ecosystems thus have the capacity to absorb a spectrum of perturbations (e.g., climate change and forest fires) and to sustain its structure and function, and to maintain the forest ecosystem in a relatively stability domain [16,17]. Climate change in the past century has caused more frequent extreme climate events, such as higher temperatures, severe, and extensive droughts [15], and also has altered forest fires regimes to varying degrees [12,18]. These changing factors (e.g., climate change and climate-induced fires) will exacerbate the loss of ecological resilience in boreal forest ecosystems under long-term exposure [15,19], and may cause a catastrophic shift in forest ecosystems that is difficult to reverse, thus posing a very serious threat to regional ecological security and forest service [20]. Therefore, understanding and quantifying ecological resilience is increasingly important for forest ecosystem management, and provides a quantitative basis for exploring the issue of maintaining and improving ecological resilience.

Harvesting and planting are major anthropogenic disturbances to boreal forests. Boreal harvesting and planting alters forest composition and structure, aboveground biomass accumulation, and ecological resilience from stand to landscape scales [21], and these effects could be aggregated under future changed climate conditions [22,23]. He et al. [22] evaluated species response to harvesting and climate-induced fire in Northern Wisconsin boreal forests, and showed that increased fire frequency can significantly alter the distribution of shade tolerant species, and indicated that harvesting accelerated the decline of Northern hardwood and boreal tree species. Gustafson et al. [23] estimated the climate effects on forest composition in the South-Central Siberian region, and indicated that the direct effects of climate change were not as important as the timber harvesting effects on local virgin forests. However,

there are fewer studies exploring the effects of forest management schemes (harvest and planting strategies) on the ecological resilience of boreal forests.

Climate change, fire disturbance, harvesting, and planting occur at large spatio-temporal scales, which makes evaluating their effects on ecological resilience using traditional observation experimental studies challenging [24,25]. Forest landscape models (FLMs) provide a proper scientific approach for studying these issues [26]. With FLMs, we can conduct large-scale studies in which critical model parameters could be changed to explore the complex interactive effects of these extra factors on ecological resilience [27].

The objective of this research was to investigate effects of climate change, climate-induced fire regimes, and future possible forest management schemes on the ecological resilience of boreal forests in Northeastern China. Specifically, we quantified (1) individual effects and (2) interactive effects of climate change and climate-induced fire disturbance on boreal forest ecological resilience, and (3) evaluated whether future possible forest management schemes could mitigate the effects of climate change and climate-induced fires on ecological resilience.

## 2. Materials and Methods

### 2.1. Study Area

The study area is located in the Great Xing'an Mountains, which covers nearly 2.7 million ha (Figure 1, 51°35' to 53°25' N and 122°25' to 125°35' E). The climate conditions are characterized by terrestrial monsoons with long winters and short summers, and the mean monthly temperatures range from −28 to 20 °C in January and July, respectively. Precipitation mainly falls in the summer, and the mean annual value is 428 mm. The elevation ranges from 173 m to 1511 m across the landscape, and the region is covered by brown coniferous forest soils. The dominant vegetation in this area is larch (*Larix gmelinii*) forests. White birch (*Betula platyphylla*) and aspen (*Populus davidiana*) are the major broad-leaved species in this region. In addition to larch and white birch, Mongolian Scots pine (*Pinus sylvestris* var. *mongolica*), and Korean spruce (*Picea koraiensis*) are also widely distributed. Dwarf pine (*Pinus pumila*) has small species communities which can be found in high latitude regions.

Forest fire is a major disturbance in the Great Xing'an Mountains. Based on the Chinese Federal Forest Service data (website: <http://www.cfsdc.org>), forest fires burned 519,144 ha of the landscape during the period of 1965 to 2005 in this region. For half a century, extreme fire suppression policies have changed fire regimes in this area profoundly. Previous studies indicated that fire regimes have changed from frequent and lower intensity fires to more infrequent and high intensity fires [28]. Extensive harvesting events have affected the forest structure, composition, and natural regeneration significantly in this region. According to the forest inventory data and our field investigation, coniferous dominated forests have shifted from late-seral to mid-seral stages over the landscape. Planting occurs rarely in our study area and overall has minimal effect compared to fire and harvesting. Under the long-term effects of these two typical disturbances (fire and harvesting), the boreal forests of our study region have become more fragmented, simplified, and less resilient [29].

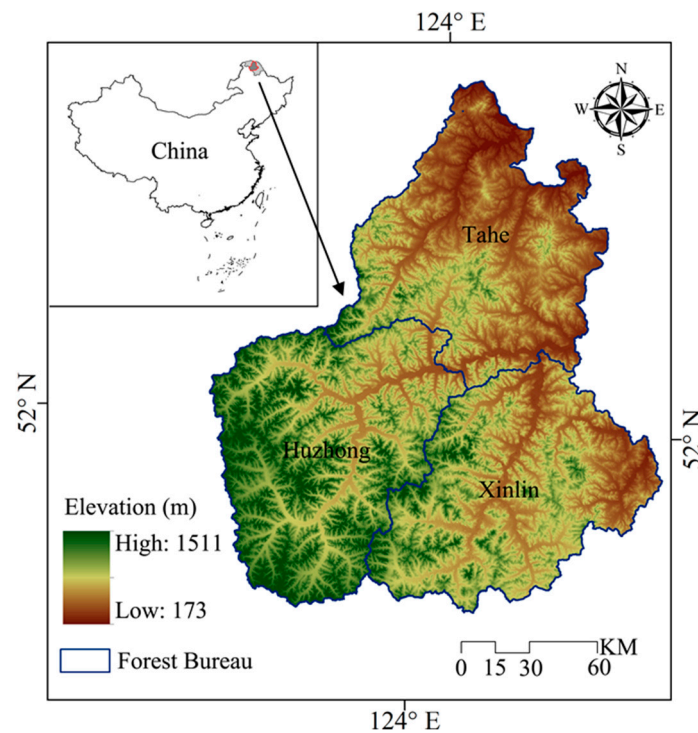


**Figure 1.** The location of our study area. The insert map shows the location of our study region in Northeastern China.

## 2.2. The Indicators of Ecological Resilience

The goal of our study was to evaluate the effects of three variables (climate change, climate-induced fire regimes and future possible forest management schemes) on ecological resilience of the study region. Firstly, by using LANDIS PRO model, we simulated the effects of climate variations, fire regimes, and forest management schemes on these four indicators: Aboveground biomass, growing space occupied, age cohort structure, and proportion of mid and late-seral species, which can be obtained directly by LANDIS PRO model outputs. Secondly, we estimated ecological resilience through these four indicators (weighted by a function of the variance). Thus, we can investigate the effects of climate variation, fire regimes, and forest management schemes on boreal ecological resilience in our study area.

Previous studies indicated that the ecological resilience can be quantified through boreal structure, composition, and functioning [15,30]. Seidl et al. [9] and Van Mantgem et al. [31] suggested that the total C storage, the rumple index, the presence of late-seral species and the proportion of older age cohorts can be served as the indicators of ecological resilience. Based on the two previous studies and the current status of our study area, we selected aboveground biomass, growing space occupied, age cohort structure and proportion of mid- and late-seral species as the indicators of ecological resilience (Table 1). The specific contents of these selected indicators are as follows: With regard to boreal forest functioning, we mainly focused on aboveground biomass (AGB). AGB plays an important role in carbon fixation, and is a vital surrogate of forest ecosystem functioning [9]. As a surrogate of forest structure, we used the growing space occupied (GSO) as an indicator of ecological resilience. The GSO is the growing space occupied by species of a specific site, and is commonly used as the crown closure measurement. Growing space primarily reflects forest structure, and can distinguish forest successional stages over large landscapes [32]. Seidl et al. [9] selected the rumple index (RI) of canopy complexity as a surrogate of vegetation structure. The rumple index is the ratio of the canopy surface area to the projected surface ground area [33]. The RI was proposed as a powerful composite index to describe vegetation structure and distinguish different stages of forest development over large areas [34], which was similar to the contents of GSO. Thus, we used GSO as the indicator of

ecological resilience in this study. The measure of GSO incorporated in LANDIS PRO is calculated by the following equations:

$$GSO_i = \sum_{j=1}^{\text{longevity/timestep}} \left( \left( \frac{DBH_j}{10 \text{ inch}} \right)^{1.605} \times NT_j \times \frac{1 \text{ hectare}}{\text{MaxSDI}_i \times \text{site\_area}} \right)$$

$$GSO = \sum_{i=1}^{\text{number of species}} GSO_i$$

where  $DBH_j$  and  $NT_j$  are the mean diameter and number of trees of  $j$  th diameter class for species  $i$  in inches and stems, respectively;  $\text{MaxSDI}$  is the maximum stand density index (derived from species vital attributes). Stand density index (SDI) is a basic concept in forestry. It was first developed by Reineke in 1933 and has been widely used to characterize stand density (tree crowding). Growing Space Occupied (GSO) represents an extension of SDI to meet the needs of landscape modeling, and is also a key metric within LANDIS PRO [32].

As a surrogate of vegetation component, we selected the percentage of older age cohort individual species (ACS). Forests which contain tree species with diverse age and size structures have been observed to be relatively more resilient to climate change and fire disturbance than forests with younger, less diverse age structures [31]. ACS is defined by the ratio of old age cohorts to the total trees cohorts (trees age > 60 year for broadleaf, and >100 year for conifers). For the surrogate of composition, we selected the proportion of mid, and late-seral species (i.e., larch, Mongolian Scots pine, and Korean spruce) >5 cm in DBH (diameter at breast height) (LSS).

**Table 1.** Indicators of forest ecological resilience.

Property	Indicators	Description	Calculation Methods
Functioning	AGB	Aboveground biomass	Derived from LANDIS PRO model outputs
Structure	GSO	Growing space occupied	The percentage of growing space on the site occupied by all species
Composition	ACS	Age cohort structure	$\frac{\text{broadleaf trees age} > 60 \text{ yr} + \text{conifer trees age} > 100 \text{ yr}}{\text{the number of all trees in each cell}}$
	LSS	Proportion of mid- and late-seral species	$\frac{\text{all conifer trees in each cell}}{\text{the number of all trees in each cell}}$

In order to facilitate the comparison and calculation among different indicators, we first used the min-max normalization method to normalize all four indicators (AGB, GSO, ACS, and LSS) by each time step at both land type and landscape scales. The data normalization process is calculated using the following Formula (1):

$$\bar{X}_i = \frac{|X_i - X_{min}|}{X_{max} - X_{min}} \quad (1)$$

where  $\bar{X}_i$  is the normalized data, which ranging from 0 to 1.  $X_i$  is the value of the indicator at year  $i$ .  $X_{min}$  and  $X_{max}$  represent the minimum and maximum values, respectively.

We then calculated the ecological resilience at all simulated time steps by using all four indicators (AGB, GSO, ACS, and LSS). The calculated ecological resilience is a specific number ranging from 0 to 1 that quantifies the capacity of different forest stands to recover from extra disturbance and maintain a stable status. Forest stands with high resilience values have a higher ability of recovery (more resilient than other stands). The formula for this is (2):

$$R_i = W_1 \times \overline{AGB}_i + W_2 \times \overline{GSO}_i + W_3 \times \overline{ACS}_i + W_4 \times \overline{LSS}_i \quad (2)$$

where  $R_i$  is the ecological resilience value at year  $i$ , higher  $R_i$  means higher ecosystem recovery ability (ecological resilience).  $\overline{AGB}_i$ ,  $\overline{GSO}_i$ ,  $\overline{ACS}_i$ , and  $\overline{LSS}_i$  represent the normalized AGB, GSO, ACS, and LSS

values at year  $i$ , respectively.  $W_j$  ( $j = 1, 2, 3, 4$ ) are the weight coefficients, which are calculated by using the coefficient of variation method in the following Formula (3):

$$W_j = \frac{\sigma_j}{\bar{X}_j \times \sum_{j=1}^n \frac{\sigma_j}{\bar{X}_j}} \quad (3)$$

where  $W_j$  is the weight coefficient of indicator  $j$ ;  $\sigma_j$  is the standard deviation of indicator  $j$ ;  $\bar{X}_j$  is the mean value of the indicator  $j$ .

### 2.3. Simulation Experiments Design and Data Analysis

We designed a factorial experiment to assess the effects of climate change, climate-induced fire regimes, and forest management schemes on boreal forest ecological resilience. In this factorial experiment, we set three independent variables: Climate change (current climate and climate change), different fire regimes (current fire and climate-induced fire), and forest management schemes (no treatment and different harvesting and planting strategies).

The current meteorological data were derived from the meteorological center, and monthly temperature and precipitation data were included from year 1961 to 2000. We used the data derived from five related weather stations to build regression models among spatial positions, elevations, and temperature as well as precipitation in the studied area. We then calculated the mean annual temperature and precipitation of different land types by using this regression model. We used two different levels of carbon emissions scenarios (CGCM3 B1 and UKMO-HadCM3 A2) to represent future climate change in our study. The B1 scenario represents low CO<sub>2</sub> emissions, while A2 represents high CO<sub>2</sub> emissions [3,35]. Based on the projected data of Hadley GCM, the mean annual temperatures and precipitations would increase linearly in year 2000–2100, and after that it would enter into a stable state [36]. The historical fire regimes for our simulations were characterized by the Chinese Federal Forest Service database from 1965 to 2005. According to previous study, fire occurrences in our study region under the B1 and A2 scenarios (projected by the Hadley GCM) would increase by 30% and 200% compared to historical fire regimes, respectively [3].

We used recent harvest trends in our study area to construct the current harvest regime. To examine the effects of the current harvest regime and future possible forest management schemes on forest ecological resilience, we designed eight harvesting and planting scenarios (Table 2). These scenarios include a combination of designated harvest intensity and increasing percentages of individual trees planted to the current intensity (P0) to 10% (P10), 20% (P20), 30% (P30), 40% (P40), and 50% (P50) of the mean stand density.

**Table 2.** The scenarios for different harvesting and planting strategies (HP) simulated by LANDIS PRO.

Scenarios	Harvesting and Planting Were Permitted	
	Harvesting Intensity for Species (H)	Planting Intensity of Conifer Trees (P)
H1P0	Cut conifer trees only	0 for each planted species
H2P0	Cut broadleaf trees only	0 for each planted species
H3P0	Cut broadleaf and conifer trees	0 for each planted species
H4P10	Cut broadleaf trees	10% for each planted conifer species
H4P20	Cut broadleaf trees	20% for each planted conifer species
H4P30	Cut broadleaf trees	30% for each planted conifer species
H4P40	Cut broadleaf trees	40% for each planted conifer species
H4P50	Cut broadleaf trees	50% for each planted conifer species

Specifically, we designed five simulated scenarios: (1) Current fire only scenario (CF1: the reference scenario, fire and succession were simulated with current fire occurrence); (2) Increased fire only scenario (CF2: compared to current fire regime, fire occurrence increased by 30%; CF3:

fire occurrence increased by 200%); (3) climate change only scenario (B1F1 and A2F1: climate change and current fire regimes were simulated); (4) climate-induced fire scenario (B1F2: B1 climate and fire occurrence increased by 30%; A2F3: A2 climate and fire occurrence increased by 200%); and (5) climate-fire-forest management schemes (B1F2HP: B1 climate, fire occurrence increased by 30% and harvesting and planting; A2F3HP: A2 climate, fire occurrence increased by 200% and harvesting and planting). We used a FLM to simulate 5 tree species (Table S1) at 5-year time step from year 2000 to 2300 with five replicates to reduce the stochasticity.

To examine the effects of extra factors on boreal forests, we compared the response variable, ecological resilience, under the reference scenario to the scenarios climate change only, increased fire only, and climate induced-fire, and climate-fire-forest management schemes for short- (0–50 year), medium- (50–150 year), and long-term (150–300 year) simulation periods using the mean comparison method. An analysis of variance (ANOVA) was used to test the differences between the reference scenario and all other scenarios. We used the Tukey’s Honestly Significant Difference (HSD) method for post-hoc analyses at all simulated periods. To evaluate the increased fire effects on boreal ecological resilience, we tested the response variable among different fire regimes at all three simulated periods. All statistical analyses were conducted using SPSS 23.0 software.

#### 2.4. Simulating Ecological Resilience from Climate Change and Disturbance

We employed a forest landscape model to simulate forest succession under different climate, fire regimes and forest management schemes, and to evaluate ecological resilience of boreal forests (Figure 2). LANDIS PRO is a spatially explicit landscape model, and can be used to simulate forest dynamic over large spatial and temporal scales with user defined resolutions (10–500 m) [34]. LANDIS PRO records density and size information for each age cohort by species within raster cells enabling the model to directly output spatially explicit stand information (e.g., density, basal area, and aboveground biomass). This data structure enables forest inventory data to be directly used for model initialization and parameterization. LANDIS PRO can simulate tree growth, species establishment, mortality, and species resources competition within each raster cell, and also simulate seed dispersal, forest management, and natural disturbance across the whole landscape. LANDIS PRO stratifies the entire landscape into relatively homogenous land type units based on climate, soil, terrain, and other environmental factors. Species establishment probability (SEP) is a key input parameter of LANDIS PRO. SEPs are obtained based on responses of each species to specific microenvironment factors such as soil moisture, soil N, soil C, and local climate. LANDIS PRO uses SEPs as inputs to indirectly capture the spatial variability of climate. Species with high SEPs have a higher probability of establishment. The SEPs of specific species are derived from previous LANDIS modeling studies or a gap model (e.g., LINKAGES).

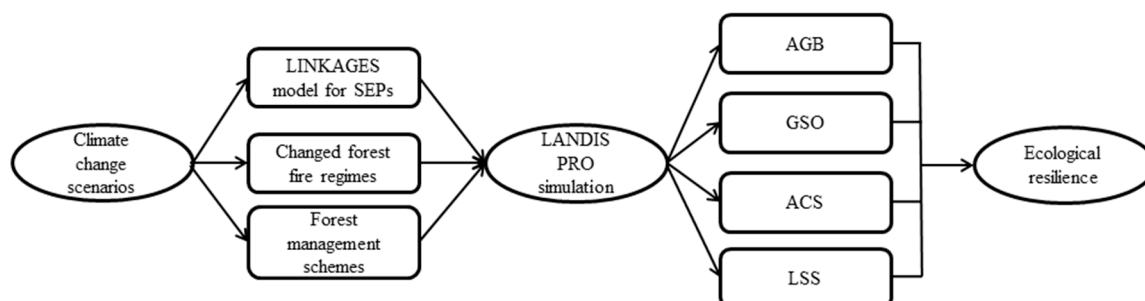


**Figure 2.** The framework for model-coupling and sub-methods used to evaluate ecological resilience. SEPs: species establishment probability, AGB: aboveground biomass, GSO: the growing space occupied, ACS: age cohort structure, and LSS: proportion of mid and late-seral species.

In the fire module, fire disturbances are simulated based on specific input parameters (e.g., mean fire return interval, mean fire sizes) [37]. Fire disturbance is simulated within spatially defined fire

regime units which have parameterized ignition rates, fire size distributions, and mean return intervals. The fire module includes three major components which are fire occurrence, fire spread, and fire effect simulation. Forest fires effects are characterized by bottom-up disturbance, and younger trees are more susceptible to fire than older ones in model simulation.

In the harvest module, forest harvesting is simulated using a management area map and forest stand map. The management area map and the stand map provide boundaries for specific harvest events to occur. Clear-cutting, thinning (from above or below), and group selection harvesting can be specified to execute harvest events in the harvest module [38]. By using those parameters, many common forest management schemes can be simulated in this module.

#### 2.4.1. LANDIS Model Initialization and Parameterization

Parameterization LANDIS PRO included two aspects: Non-spatial parameters (species' vital attributes, SEPs, site-level fire disturbance, harvest scenarios, and planting parameters), and spatial parameters (species composition map, land type map, management area map, stand map, and fire regime unit map). Five of the most common tree species were simulated in LANDIS, which account for more than 90% of the total forested land [29]. Species' vital attributes were derived from previous studies in the same or similar regions, field investigation, and consultation with local experts [39,40]. We used land use data, Landsat imagery, slope, and aspect maps to classify the study area landscape into six land types. We then used LINKAGES to simulate the response of forest species under current and climate change scenarios within each land type, and used the simulated individual species biomass to estimate SEPs for each simulated species. We modeled the SEPs of five tree species under different climate conditions by each land type (Table 3). The initial SEPs were estimated by current climate (1961–2000), and the SEPs for future scenarios were projected by climate change data (2010–2099). The SEPs were assumed to change linearly in 2000–2100, and held constant after 2100. Specifically, we used LINKAGES to simulate the individual biomass of different tree species to both current and climate warming scenarios within each land type. The individual species biomass was used to estimate the SEPs for specific species. The SEPs are calculated by the following equation:

$$SEP_{ij} = \frac{b_{ij}, b'_{ij}}{\max\left\{\sqrt{\sum_{j=1}^n b_{ij}}, \sqrt{\sum_{j=1}^n b'_{ij}}\right\}}$$

where  $b_{ij}$  and  $b'_{ij}$  are the biomass of species  $i$  on land type  $j$  under current and warmer climate, respectively,  $SEP_{ij}$  is the species establishment probability of species  $i$  on land type  $j$  under current and warming climate [36,41].

The forest composition map was obtained based on forest stand maps, forest inventory data, and field data, which included species spatial location, number of trees and age cohort information. The forest stand map was acquired in the 2000's was a GIS based file, that provided stand site boundaries, species composition, structure, and the average age of the specific polygons. We derived sample plots investigated during the 2000's, which provided number of trees and age cohorts by species from the China National Forest Inventory Second and Third Tier data. We integrated the forest stand map (vector format) and forest inventory data (stand information) to derive the initial forest composition map. To reduce computational resources, all those input maps needed by LANDIS model were converted to a resolution of 90 m × 90 m cell size (2217 columns × 2609 rows) by using ESRI ArcGIS software.

Fire regime parameters and a fire regime unit map were required for the fire module. The fire regime unit map was used to identify areas with heterogeneous fire properties across the landscape, and fire characteristics in this region were mostly related to soil moisture, terrain, climate, and vegetation traits, which were closely related to the classification of land types, and thus we used the land type map as the fire regime unit map in our study area. The current fire occurrence for our simulations was parameterized based on data from the historical fire database recorded from 1965 to

2005. Based on the database, we calculated the current fire regime parameters (e.g., return interval, ignition rate, and mean fire size) of each fire regime unit. The future fire regimes were characterized by changing fire occurrences under different climate scenarios based on previous work [3]. The boreal forests in our study area have been exploited since the 1950's, and timber harvesting has extensively altered forest composition, structure, and age cohort. Consequently, to maintain forest ecosystem function and sustainability, timber harvesting has been restricted by a natural forest conservation project since 1999. Mongolian Scots pine and Korean spruce were extensively cut because of their high economic value and stands typically reestablished with larch. At present the local forestry bureaus have attempted to actively protect the remaining stock of these two species. In accordance with current harvest policy, the harvested species were larch, birch, and aspen, whereas pine and spruce were not harvested. The predominant harvest type in our study area was thinning from below, and all harvest scenarios were processed by removing the smallest trees first. We simulated the current harvest activities by using a basal area controlled harvest method (tree species were removed from a stand until a specific target basal area value was reached) followed by planting in permitted areas.

**Table 3.** SEPs for each available land type under current climate and climate change scenarios.

Land Type	Climate Scenario <sup>1</sup>	Species Establishment Probabilities (SEPs)				
		Larch	Pine	Spruce	White Birch	Aspen
Terrace	C	0.200	0.050	0.050	0.030	0.070
	B1	0.060	0.200	0.180	0.076	0.166
	A2	0.000	0.000	0.000	0.418	0.186
Southern slope	C	0.350	0.350	0.005	0.350	0.030
	B1	0.376	0.327	0.174	0.284	0.106
	A2	0.141	0.320	0.111	0.669	0.271
Northern slope	C	0.400	0.010	0.030	0.150	0.005
	B1	0.522	0.406	0.388	0.190	0.042
	A2	0.270	0.151	0.245	0.238	0.213
Ridge top	C	0.200	0.010	0.000	0.070	0.020
	B1	0.346	0.100	0.020	0.076	0.010
	A2	0.413	0.325	0.180	0.222	0.147

<sup>1</sup> C: current climate condition; B1 and A2: climate change scenarios.

#### 2.4.2. Model Calibration and Verification

Simulated results (e.g., species composition, tree density, basal area, and aboveground biomass by species for each cell and time-step) from LANDIS PRO can be directly compared with forest inventory data as a method of calibration and validation [32]. In order to parameterize the initial forest landscape accurately, we used 70% of the inventory plots (investigated in 2000s, consists of the number of all trees and age cohorts) and the stand map (a GIS file) to initialize the forest composition map at year 2000, and then simulated the model for ten years. We iteratively adjusted species' growth curve (an essential input parameter used to control tree growth and calculate species biomass) to make the initialized forest stand information match the remaining 30% of the forest inventory data at year 2000. We then calibrated the number of potential established seeds (a parameter related to tree density and basal area) until the simulated results for year 2010 was similar to field data for the year 2010. This calibration ensured that species' growth curves and the number of potential established seeds was suitable for our study area [39]. To evaluate the simulated landscape at year 2010, we used a scatter plot of the observed density and basal area vs. the simulated density and basal area. We first selected 322 raster cells from the simulated landscape at year 2010, and then the density and basal area were extracted from selected cells to compare with forest inventory data. Likewise, the forest inventory data (322 plots, investigated in 2010s) were also converted to the total density and basal area.

To verify simulated fire on the forested landscape, we compared the model results with field data at different simulated periods. We ran the current fire only scenario (CF1) for 300 years, and randomly

selected 40 fires with low intensities (more than 90% fires occurred at this level in our study area) from different years and locations from the LANDIS PRO output. We then inventoried 40 field sites (8 field sites per each age group) that were actually burned 5, 10, 15, 20, and 25 before the year they were sampled. We set five plots with 20 m  $\times$  20 m in each field site. We then recorded all the individual trees with basal diameter above 1 cm level in each plot. Tree number and DBH by species were measured at each plot, and these plot data were converted to density (trees/ha) and basal area ( $m^2/ha$ ). We statistically compared tree density and basal area of the 40 simulated fires with 40 corresponding fires sampled in the field, respectively.

To ensure the simulated results more authentic, we also compared the simulated aboveground biomass to previous studies, which conducted plot surveys in similar region at landscape scales. We used the currently available data for model evaluation. While predicted results under climate change scenarios over next 280 years cannot be verified by field inventory data, simulated successional and stand dynamic trends have been confirmed by other studies conducted at similar regions [36,42].

### 3. Results

#### 3.1. Model Calibration and Validation

Our simulated results indicated that the initialized forest composition constructed from the observed data from year 2000 adequately represented the forest landscape (stand density:  $R^2 = 0.821$ , Pearson correlation test:  $p < 0.01$ ; basal area:  $R^2 = 0.804$ ,  $p < 0.01$ ) (Figure 3a,b). The simulated stand density and basal area were close to the observed forest inventory data at year 2010 (stand density:  $R^2 = 0.803$ ,  $p < 0.01$ ; basal area:  $R^2 = 0.832$ ,  $p < 0.01$ ) (Figure 3c,d). Thus, we accepted the calibrated results for further calculation.

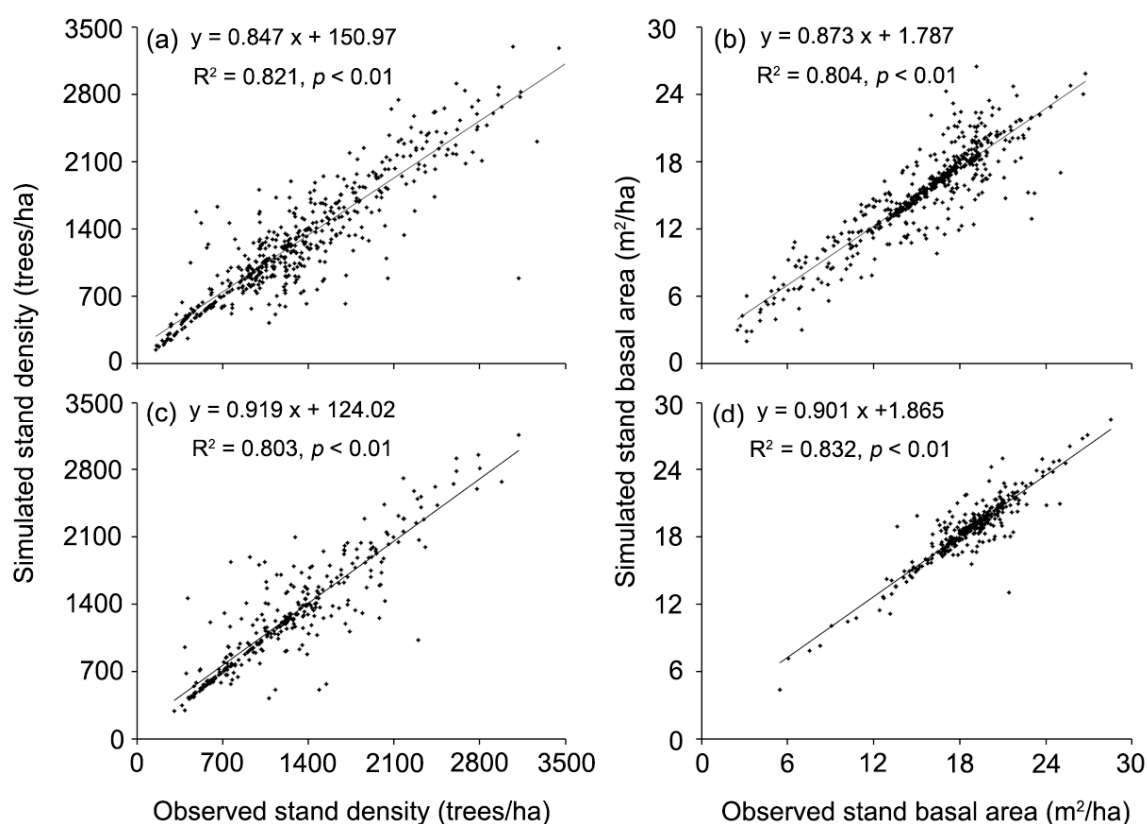


**Figure 3.** Scatter plot showing the relation between simulated and observed data for stand density (a,c); and basal area (b,d) at year 2000 and 2010, respectively (Pearson correlation test:  $p < 0.01$ ).

The results showed that the post-fire stand density increased during the first 10 years (up to 17,295 trees/ha) and then decreased to 4725 trees/ha after 25 years (Figure 4a). The increasing trend was largely attributed to forest fires removing many trees causing the release of growing space for pioneer species to establish. After year 10, these post-fire stands reached the self-thinning stage, and began to reduce individual trees in the following years. The post-fire basal area showed an increasing trend throughout the observed 25 years (Figure 4b). The simulated trends in both stand density, basal area and aboveground biomasses closely followed trends in the field sample data (Figures 4 and 5).

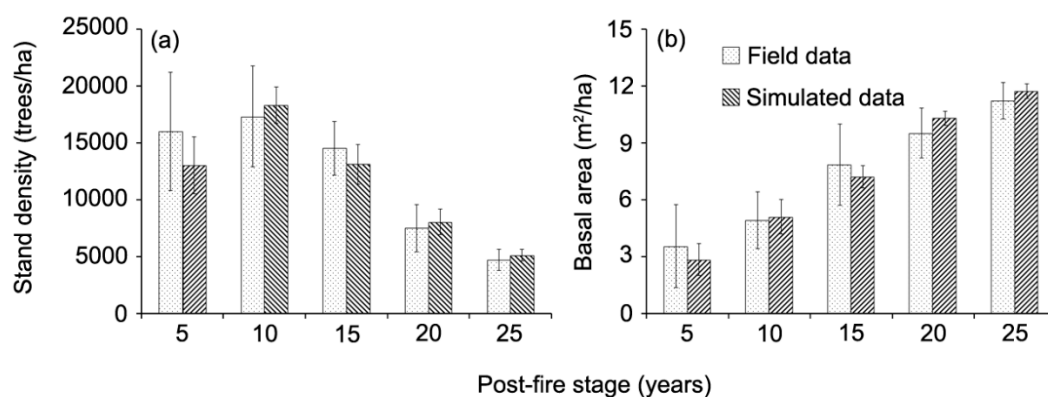


**Figure 4.** Comparison between observed and simulated stand density (a) and basal area (b) in burned areas in relation to post-fire year.

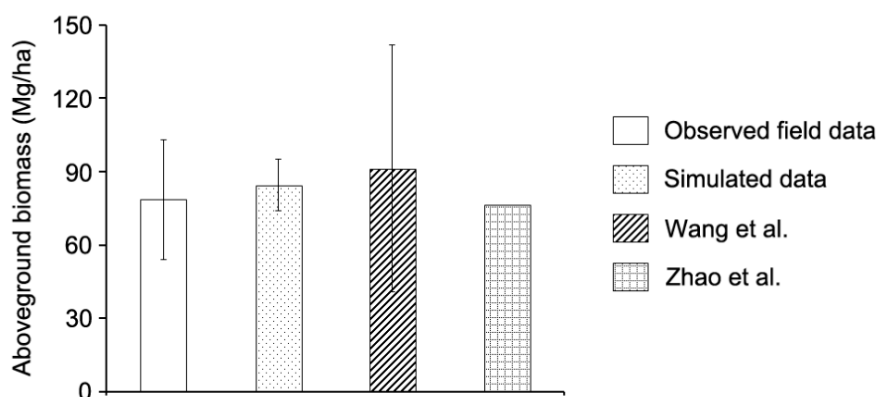


**Figure 5.** Comparison between simulated data and observed field aboveground biomass, published data from plot surveys in the study area.

### 3.2. Ecological Resiliencies Response to Climate Change and Fire Regimes at Landscape Scale

Our results showed that under current climate conditions, ecological resilience was affected by forest fire regimes (Figure 6a). The forest ecological resilience was greatest under the CF2 scenario followed by the CF1 and CF3 scenarios. Under the current fire regimes (CF1), the ecological resilience increased rapidly from the simulated years 50 to 80, then decreased until year 160, and then increased slightly to year 300. The ecological resilience decreased significantly under the CF3 scenario in the first 160 years compared to the CF1 scenario. However, the ecological resilience under CF1 scenario coincided with the CF3 scenario from year 170 to 270.

The trajectories of forest ecological resilience varied among climate change and fire regime scenarios (Figure 6b). Under B1F1, B1F2, and A2F1 scenarios, the ecological resilience dynamics had a similar trend for the whole simulation period. The curves of these three scenarios fluctuated in the first 50 years and peaked at year 80, then decreased until year 160, and then increased to year 300 gradually. The calculated forest ecological resilience was highest under the B1F2 scenario across all simulated

periods, followed by B1F1, A2F1, and A2F3 scenarios. Moreover, the ecological resilience under the A2F3 scenario was visibly lowest among these scenarios until year 210.

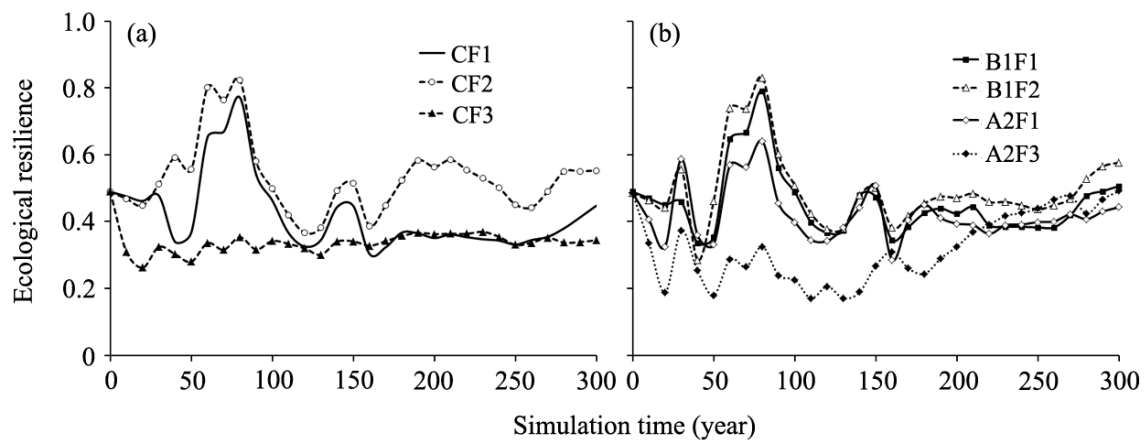


**Figure 6.** Changes in ecological resilience at the landscape level under different simulated scenarios. (a) current climate condition with different fire occurrence (CF1, CF2, and CF3); and (b) climate change scenarios with different fire occurrences (B1F1, B1F2, A2F1, and A2F3).

### 3.3. Effects of Fire Regimes, Climate Change on Ecological Resilience

The effects of forest fire on ecological resilience varied among the three fire occurrence scenarios across the three simulated periods (Figure 7). Compared to the CF1 scenario, no significant difference was found between the short and medium term interval ( $p > 0.05$ ) under CF2 scenario, while the ecological resilience under the CF2 scenario differed significantly from CF1 scenario during long-term interval ( $p < 0.05$ ). However, the ANOVA tests demonstrated that the simulated ecological resilience under CF3 scenario for both short and medium term interval differed significantly from CF1 scenario ( $p < 0.05$ ), and no significant difference existed in the long term interval (150–300 year).

The ecological resilience was substantially higher under the CF2 scenario than the CF1 scenario (Figure 7). Our results showed that the increase in ecological resilience under CF2 scenario was 17.5%, 12.4%, and 43.2% greater than that in CF1 scenario across the entire simulated periods, respectively. Under CF3 scenario, the largest reduction in ecological resilience occurred in the short and medium term interval, and was 24.6% and 34.3% lower than that in the CF1 scenario. However, the average value of ecological resilience under CF3 scenario was similar in the long-term period.

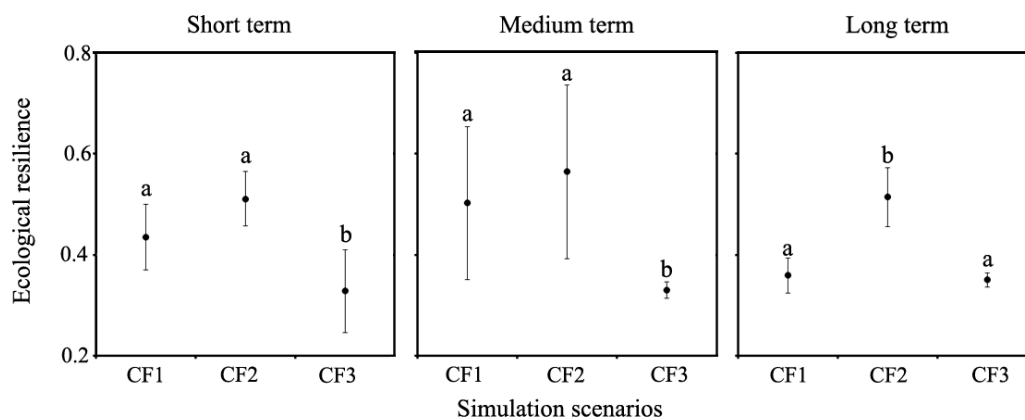


**Figure 7.** Multiple comparison of three fire scenarios effects on ecological resilience at different simulated periods. Small letters indicated significant differences among scenarios at 0.05 level. CF1, CF2, and CF3: different fire occurrence scenarios.

The ecological resilience responses to three climatic scenarios differed among different land types (Figure 8). Results showed that the ecological resilience increased more sharply in the first 80 years (up to 0.919), then decreased until year 170, and then increased slightly to year 300, and the ecological resilience responded negatively to both B1, A2 climate scenarios after year 80 on the terrace land type (Figure 8a). On south-facing slopes, the ecological resilience decreased in the first 50 years, then increased slightly until year 80, and remained almost stable afterward under the CF1 and B1F1 scenarios. Ecological resilience under A2F1 scenario decreased by 61.5% in the first 130 years, and then generally increased to year 300 (Figure 8b). The curves of ecological resilience in north-facing land type responded to climate change similar to that on south-facing land types (Figure 8c). On the ridge top land type, the curves of ecological resilience under three climatic scenarios decreased sharply in the first 30 years, and then increased slightly afterward (Figure 8d). There was a slight increase of ecological resilience in B1F1 and A2F1 scenarios compared to the CF1 scenario after year 120 (Figure 8e).

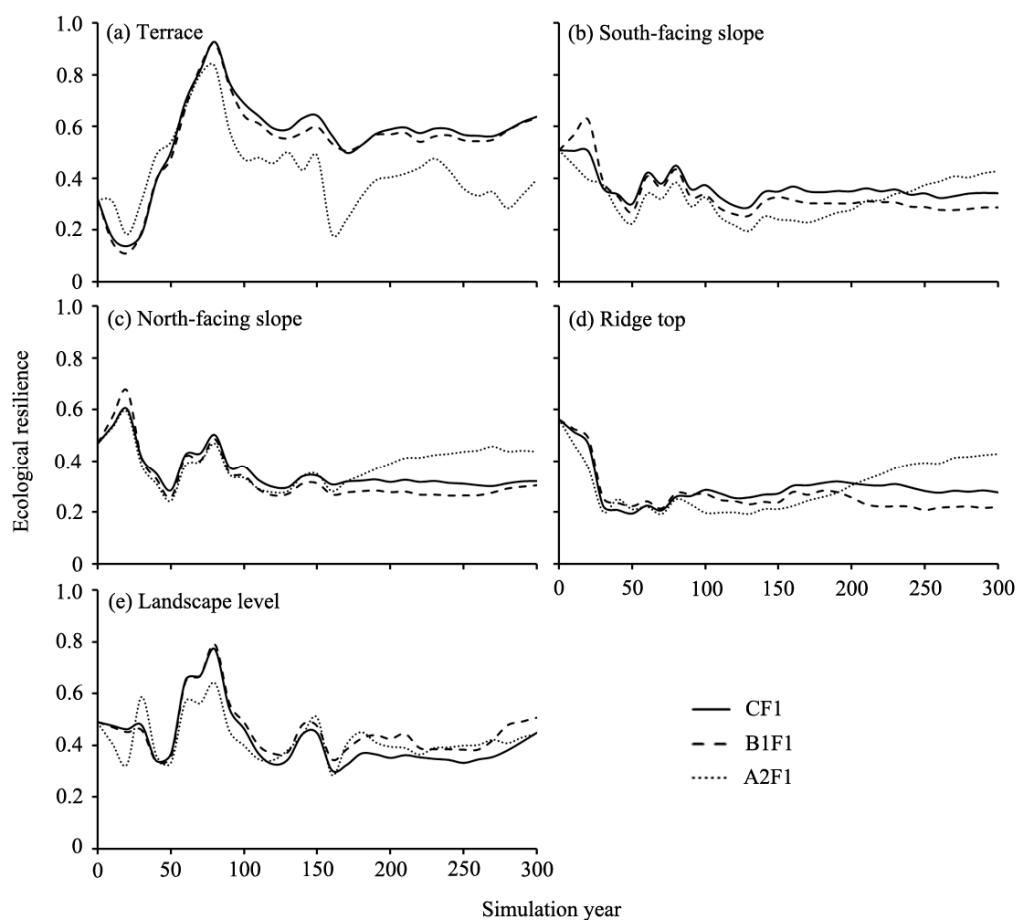


**Figure 8.** Ecological resilience dynamics for different land types under three climatic simulated scenarios. CF1: current fire only scenario, and B1F1, A2F1: climate change only scenarios.

### 3.4. The Interactive Effects of Fire Disturbance and Climate Change on Ecological Resilience

There was no significant difference of ecological resilience on the terrace land type between CF1 and B1F2 scenarios during the simulated periods ( $p > 0.05$ , Figure 9); and ecological resilience on the terrace land type decreased by 1.7%, 5.9%, and 1.7% at the three simulated periods compared to the CF1 scenario. For the South-facing and North-facing land types, the ecological resilience did not differ significantly between CF1 and B1F2 scenarios for the short and medium-term interval ( $p > 0.05$ , Figure 9). However, ecological resilience differed significantly between the B1F2 scenario and the CF1 scenario for the long-term period ( $p < 0.05$ , Figure 9), where ecological resilience was 11.3% lower than

that in CF1 scenario. On the ridge top land type, no significant difference was found between CF1 and B1F2 scenarios for the whole simulation periods, where ecological resilience was 14.1% higher, and 3.7% lower, respectively, than that in the CF1 scenario. The results showed that ecological resilience under the B1F2 scenario was significantly higher than that under CF1 scenario at landscape scale only for the long-term period ( $p < 0.05$ , Figure 9). The increase in ecological resilience at the landscape scale was 3.2%, 12.1%, and 29.6% greater than that in the CF1 scenario during the three simulated periods, respectively.

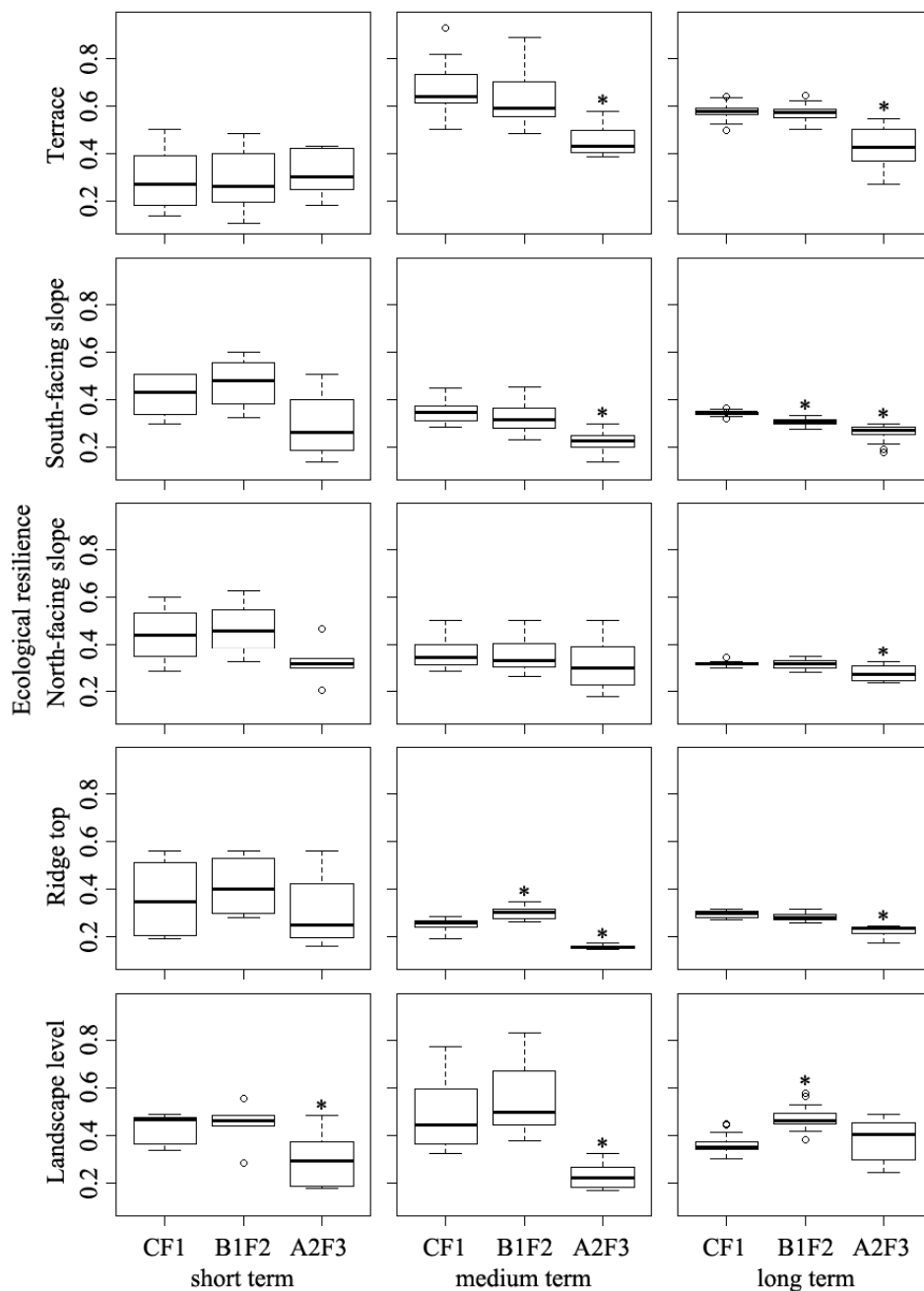


**Figure 9.** Ecological resiliencies of different land types for the three simulated scenarios: current fire only scenario (CF1); climate change induced-fire scenarios (B1F2, A2F3). Short term: 0–50 years, medium term: 50–150 years, and long term: 150–300 years; \* indicates that significant differences are detected between the CF1 scenario and a given scenario ( $p < 0.05$ ).

Ecological resilience under the A2F3 scenario differed significantly on terrace, South-facing slope, and ridge top land types from CF1 scenario at medium and long-term periods ( $p < 0.05$ , Figure 9), and no significant differences were detected at short-term interval on those three land types. On North-facing slopes, the ecological resilience under A2F3 scenario differed significantly from CF1 scenario during the long-term period ( $p < 0.05$ , Figure 9), and the decrease in ecological resilience was 26.7%, 12.4%, and 12.3% lower than that in the CF1 scenario across the three simulated periods, respectively. Collectively, our results indicated that the B1F2 scenario did not affect ecological resilience across the short- to medium-term range, but with continuous climate and fire influence, it will significantly affect the ecological resilience at landscape level across the long-term range. Meanwhile, under the A2F3 scenario, forest ecological resilience could be recovered almost to its original state by 150 years simulation time.

### 3.5. The Effects of Forest Management Schemes on Ecological Resilience

Our results showed that forest management schemes played a role in altering ecological resilience under the climate change scenarios in contrast to the no management treatments (Figure 10). For the B1F2 scenario, ecological resilience decreased obviously under the eight harvesting and planting scenarios (Figure 10a). Under all simulated scenarios, ecological resilience initially fluctuated, then peaked at year 80, and then decreased until year 130, and increased gradually afterward. The curves of ecological resilience for the eight harvesting and planting scenarios were relatively lower than that under B1F2 scenario during most of the simulation periods. Generally, our results indicated that all eight harvesting and planting strategies did not affect ecological resilience at landscape scale under the B1F2 scenario during all simulation periods.

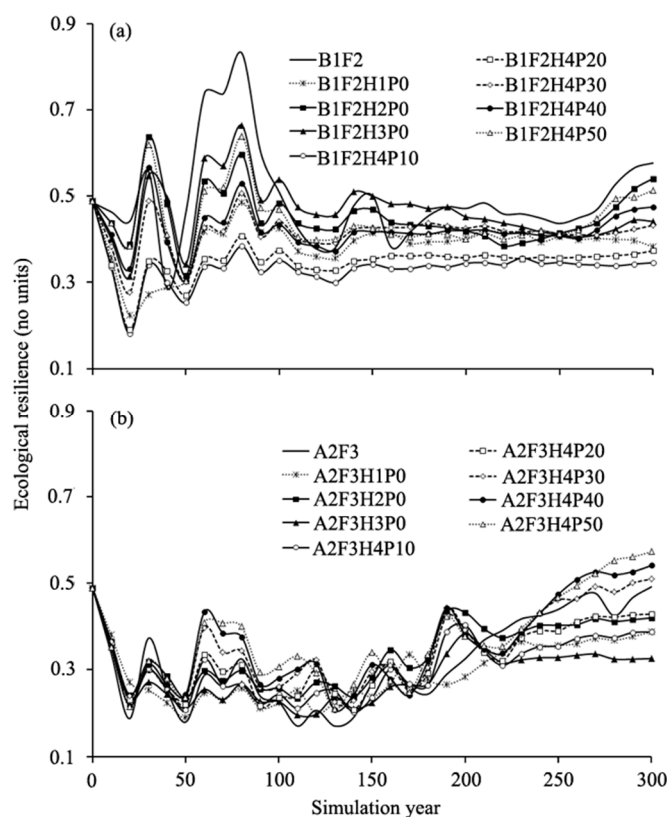


**Figure 10.** The ecological resilience simulated under different forest management schemes at landscape scales under two climate change scenarios in comparison with no management treatment (B1F2 and A2F3): (a) The ecological resilience affected by harvesting and planting in B1 climatic scenario; and (b) the ecological resilience affected by harvesting and planting in A2 climatic scenario.

For the A2F3 scenario, ecological resilience also varied among these eight harvesting and planting strategies across all simulation periods (Figure 10b). Ecological resilience decreased sharply under all the harvesting and planting scenarios in the first 20 years, and then fluctuated until year 220 and increased gradually afterward. The ecological resiliencies of eight harvesting and planting scenarios were higher than that under A2F3 scenario during the first 190 years simulation. Under A2F3H4P30, A2F3H4P40, and A2F3H4P50 scenarios, the ecological resiliencies were higher than that under the A2F3 scenario after year 240 (Figure 10b). Our results indicated that certain harvesting and planting strategies needed to be implemented under the A2F3 scenario, and only three of the eight harvesting and planting strategies affected the ecological resilience positively at the landscape level during the simulation periods except for simulated year 210 to 240.

#### 4. Discussion

Boreal forest ecosystems have the ability to recover from disturbances without undergoing fundamental change (a quality referred to as resilience) that it is dependent on functions and structures at multiple scales of the forest ecosystem [15,43]. Understanding and quantifying responses of ecological resilience to extra disturbances is a challenge [44] because ecological resilience dynamics are an inherent ecosystem property that is related to multiple scales and comprehensive spatiotemporal data does not exist, and further cannot be feasibly measured directly by field observations [16,45]. Ecological resilience can be estimated by means of ecological resilience indices such as biodiversity, habitat conditions, and productivity etc., and many studies had been focused on this issue [10,46,47]. For example, Scheffer et al. [20] suggested that maintaining the ecological resilience of forest ecosystems was likely be the most feasible and effective way to manage forest ecosystems under possible future changing environments. Chapin et al. [15] assessed the resilience of boreal forest ecosystems to rapid climate change. In contrast to those studies, the spotlight of our study lies in the quantitative parts and resilience prediction. To our knowledge, few previous studies have used resilience indicators to calculate the ecological resilience at a landscape scale, and evaluate the effects of climate change and fire regimes on the ecological resilience at both land type and landscape scales. In our research, we used a FLM to evaluate the ecological resilience of forests to climate change and altered fire regimes. This modeling approach can be used to further explore these broad-scale issues, and to evaluate the interactions of forest succession and disturbance dynamics. Furthermore, it provides long term insights in exploring forest ecological resilience. The LANDIS PRO model can explicitly track aboveground biomass, species composition, tree number, and age cohorts, which can be verified by directly comparing to the field data. The validation process conducted in our study added to the robustness of our modeling approach and confidence of predictions (Figures 3–5). To verify the aboveground biomass indicator, we compared our results with field data and published data in the same or similar regions. The results showed that the predicted aboveground biomass ( $84.9 \pm 10.6 \text{ Mg/hm}^2$ ) were within the observed ranges of the field sample data we collected ( $78.5 \pm 24.4 \text{ Mg/hm}^2$ ) and the published data reported by Wang et al. [48] ( $91.4 \pm 50.4 \text{ Mg/hm}^2$ ) and Zhao et al. [49] ( $76.5 \text{ Mg/hm}^2$ ), respectively (Figure 5). Utilizing the full range of outputs from the LANDIS PRO model make it possible to further explore the dynamics of ecological resilience, and to assess the effects of climate change, climate-induced fire regimes, and forest management schemes.

Ecological resilience was enhanced under the low fire occurrence scenario in comparison to the current fire occurrence condition, whereas it decreased under the high fire occurrence scenario (Figure 7). This suggested that low fire occurrence had positive effects on boreal forest's resilience, while high fire occurrence should be avoided in future forest management. However, previous studies showed that low fire occurrences had negative effects on boreal forest ecosystem resilience [36,50]. This difference may be related to response variable selection or analysis of fewer indicators of ecological resilience. Meanwhile, the curve of ecological resilience under the CF2 scenario increased in the first 80 years and decreased in the next 50 years. This was likely because low-intensity forest fires removed mostly small trees and released growing space for white birch and aspen to recruit. After the process

of post-fire tree recruitment progressed over the first 70 to 80 years, self-thinning began to cause mortalities of pioneer species over the next 50 years. Meanwhile, many of these pioneer trees had reached their longevity and began to die in the self-thinning process [51].

Our results revealed that ecological resilience under climate change scenarios changed differently among simulated land types. Under climate change only scenarios, the curves of ecological resilience were slightly lower than that under current fire only scenario among different land types during different simulated periods (Figure 8). This may have been related to the variation in species establishment probabilities among climate scenarios at different land types, and the initial forest composition and tree distribution [22,52]. Within the terrace land type, the ecological resilience was significantly lower under A2F1 scenario than that under CF1 and B1F1 scenarios after year 80 (Figure 8a). This was because most of the terrace land type area was covered by coniferous species with trees in middle-age cohorts, and the present-day dominant larch trees could not establish under A2 climate scenario [29]. There was a time lag for the effects of climate change and fire disturbance on ecological resilience among different land types (Figure 9). This was consistent with previous studies [36,53]. Furthermore, our simulated results indicated that time lags were varied among different land types under climate change scenarios. For instance, the response time of ecological resilience to A2F3 scenario was 150 years in North-facing slope region, which was almost 100 years longer than that in the South-facing slope land type, and this discrepancy may related to the distribution patterns of solar energy and available water resources in future climate change scenarios between these two land types, and the current coniferous and broadleaf species distribution [54].

Forest management schemes played an important role in influencing ecological resilience under climate change scenarios at the landscape level (Figure 7). Our results showed that many of the harvesting and planting strategies had negative effects on the ecological resilience compared to the B1F2 scenario. There were two reasons for this: (1) Fire regimes under B1F2 scenario removed many small trees, and released growing space for species to occupy. Meanwhile, the thinning methods of harvesting also removed most small broadleaf trees; (2) Due to shortages of growing space, planting efficiency of coniferous trees was relatively low, and the planted trees did not offset total removals due to fire and harvest events [29]. In this light, we concluded that no additional forest management treatments were suitable under the future B1F2 scenario. Our results moreover showed that most of the harvesting and planting strategies had positive effects on ecological resilience, and the curves of ecological resilience under A2F3H4P30, A2F3H4P40, and A2F3H4P50 scenarios were obviously higher than that under the A2F3 scenario in most of the simulated periods. This may have been related to the influences of changed environmental conditions under A2 climate scenario, increased fire occurrence, and the different biophysical limits of coniferous and broadleaf trees when facing future changing climates [55]. This suggested that the three of eight strategies were suitable under the future A2F3 scenario.

## 5. Conclusions

In this study, we predicted the dynamics of forest ecological resilience indicators (AGB, GSO, ACS, and LSS) at both landscape and land type scales in boreal forests by employing a forest landscape model, and then quantified the ecological resilience by incorporating those representative indicators. This modeling approach also provided insight into ecological resilience trends under changing climate conditions, fire regimes and possible future forest management schemes. In conclusion, we found that: (1) The LANDIS PRO model can be implemented in evaluating ecological resilience of boreal forests at multi scales in Northeastern China; (2) the ecological resiliencies of forests in the Great Xing'an mountains were likely to be significantly altered by different climate conditions, fire regimes, and their interactive effects during most of the simulated periods; (3) the direct effects of climate variations on forest ecological resilience in the study area are not likely to be as important as the possible changed fire regimes at the landscape scale, and future climate warming (high CO<sub>2</sub> emission) with high fire occurrence regime would significantly reduce the ecological resilience of forest ecosystem;

(4) the proposed forest management schemes do not mitigate the effects of climate variation and climate-induced fire regime effects under the low climate-induced fire regime scenario, and medium and high intensities of forest management schemes (30%, 40%, and 50% intensities) are proposed under the high climate-induced fire regime scenario. These results provided useful information for future boreal forest managements.

**Supplementary Materials:** The following are available online at <http://www.mdpi.com/2071-1050/10/10/3531/s1>, Table S1: Main species attributes of our study landscape.

**Author Contributions:** X.L. and H.S.H. designed the simulated scenarios, analyzed the data and wrote this manuscript; J.S.F. helped with the harvest module runs; Y.L. greatly improved the experimental design and the manuscript. J.L. supervised the analysis and figure design.

**Funding:** This research was funded by the National Natural Science Foundation of China (Nos. 31600373 and 41371199) and the K.C. Wong Magna Fund of Ningbo University.

**Acknowledgments:** We'd like to thank the workgroup from the three Forestry Bureaus for providing details on current forest management and field investigations.

**Conflicts of Interest:** The authors declare no conflict of interest.

## References

- Bhatti, J.S.; Van Kooten, G.C.; Apps, M.J.; Laird, L.D.; Campbell, I.D.; Campbell, C.; Turetsky, Z.Y.; Banfield, E. Carbon balance and climate change in boreal forests. In *Towards Sustainable Management of the Boreal Forest*; NRC Research Press: Ottawa, ON, Canada, 2003; pp. 799–855.
- Euskirchen, E.S.; McGuire, A.D.; Chapin, F.S.; Rupp, T.S. The changing effects of Alaska's boreal forests on the climate system. *Can. J. Forest. Res.* **2010**, *40*, 1336–1346. [[CrossRef](#)]
- Liu, Z.; Yang, J.; Chang, Y.; Weisberg, P.J.; He, H.S. Spatial patterns and drivers of fire occurrence and its future trend under climate change in a boreal forest of Northeast China. *Glob. Chang. Biol.* **2012**, *18*, 2041–2056. [[CrossRef](#)]
- Weber, M.G.; Flannigan, M.D. Canadian boreal forest ecosystem structure and function in a changing climate: Impact on fire regimes. *Environ. Rev.* **1997**, *5*, 145–166. [[CrossRef](#)]
- Xu, C.G.; Gertner, G.Z.; Scheller, R.M. Potential effects of interaction between CO<sub>2</sub> and temperature on forest landscape response to global warming. *Glob. Chang. Biol.* **2007**, *13*, 1469–1483. [[CrossRef](#)]
- Kelly, A.E.; Goulden, M.L. Rapid shifts in plant distribution with recent climate change. *Proc. Natl. Acad. Sci. USA* **2008**, *105*, 11823–11826. [[CrossRef](#)] [[PubMed](#)]
- Lloyd, A.H.; Bunn, A.G.; Berner, L. A latitudinal gradient in tree growth response to climate warming in the Siberian taiga. *Glob. Chang. Biol.* **2011**, *17*, 1935–1945. [[CrossRef](#)]
- Stueve, K.M.; Isaacs, R.E.; Tyrrell, L.E.; Densmore, R.V. Spatial variability of biotic and abiotic tree establishment constraints across a treeline ecotone in the Alaska Range. *Ecology* **2011**, *92*, 496–506. [[CrossRef](#)] [[PubMed](#)]
- Seidl, R.; Rammer, W.; Spies, T.A. Disturbance legacies increase the resilience of forest ecosystem structure, composition, and functioning. *Ecol. Appl.* **2014**, *24*, 2063–2077. [[CrossRef](#)] [[PubMed](#)]
- Medlyn, B.E.; Duursma, R.A.; Zeppel, M.J.B. Forest productivity under climate change: A checklist for evaluating model studies. *Wires. Clim. Chang.* **2011**, *2*, 332–355. [[CrossRef](#)]
- Johnstone, J.F.; Hollingsworth, T.N.; Chapin, F.S.; Mack, M.C. Changes in fire regime break the legacy lock on successional trajectories in Alaskan boreal forest. *Glob. Chang. Biol.* **2010**, *16*, 1281–1295. [[CrossRef](#)]
- Flannigan, M.; Stocks, B.; Turetsky, M.; Wotton, M. Impacts of climate change on fire activity and fire management in the circumboreal forest. *Glob. Chang. Biol.* **2009**, *15*, 549–560. [[CrossRef](#)]
- Wotton, B.M.; Nock, C.A.; Flannigan, M.D. Forest fire occurrence and climate change in Canada. *Int. J. Wildland Fire* **2010**, *19*, 253–271. [[CrossRef](#)]
- Soja, A.J.; Tchekakova, N.M.; French, N.H.F.; Flannigan, M.D.; Shugart, H.H.; Stocks, B.J.; Sukhinin, A.I.; Parfenova, E.I.; Chapin, F.S.; Stackhouse, J.P.W. Climate-induced boreal forest change: Predictions versus current observations. *Glob. Planet. Chang.* **2007**, *56*, 274–296. [[CrossRef](#)]

15. Chapin, F.S.; McGuire, A.D.; Ruess, R.W.; Hollingsworth, T.N.; Mack, M.C.; Johnstone, J.F.; Kasischke, E.S.; Euskirchen, E.S.; Jones, J.B.; Jorgenson, M.T.; et al. Resilience of Alaska's boreal forest to climatic change. *Can. J. For. Res.* **2010**, *40*, 1360–1370. [[CrossRef](#)]
16. Holling, C.S. *Engineering Resilience Versus Ecological Resilience*; National Academy Press: Washington, DC, USA, 1996; pp. 31–44.
17. Peterson, G.; Allen, C.R.; Holling, C.S. Ecological resilience, biodiversity, and scale. *Ecosystems* **1998**, *1*, 6–18. [[CrossRef](#)]
18. Running, S.W. Is global warming causing more, larger wildfires? *Science* **2006**, *313*, 927–928. [[CrossRef](#)] [[PubMed](#)]
19. Turner, M.G. Disturbance and landscape dynamics in a changing world. *Ecology* **2010**, *91*, 2833–2849. [[CrossRef](#)] [[PubMed](#)]
20. Scheffer, M.; Carpenter, S.; Foley, J.A.; Folke, C.; Walker, B. Catastrophic shifts in ecosystems. *Nature* **2001**, *413*, 591–596. [[CrossRef](#)] [[PubMed](#)]
21. Yao, J.; He, X.Y.; He, H.S.; Chen, W.; Dai, L.M.; Lewis, B.J.; Yu, L.Z. The long-term effects of planting and harvesting on secondary forest dynamics under climate change in northeastern China. *Sci. Rep.* **2016**, *6*, 18490. [[CrossRef](#)] [[PubMed](#)]
22. He, H.S.; Mladenoff, D.J.; Gustafson, E.J. Study of landscape change under forest harvesting and climate warming-induced fire disturbance. *For. Ecol. Manag.* **2002**, *155*, 257–270. [[CrossRef](#)]
23. Gustafson, E.J.; Shvidenko, A.Z.; Sturtevant, B.R.; Scheller, R.M. Predicting global change effects on forest biomass and composition in south-central Siberia. *Ecol. Appl.* **2010**, *20*, 700–715. [[CrossRef](#)] [[PubMed](#)]
24. He, H.S.; Yang, J.; Shifley, S.R.; Thompson, F.R. Challenges of forest landscape modeling—Simulating large landscapes and validating results. *Landsc. Urban Plan.* **2011**, *100*, 400–402. [[CrossRef](#)]
25. Gustafson, E.J.; Shvidenko, A.Z.; Scheller, R.M. Effectiveness of forest management strategies to mitigate effects of global change in south-central Siberia. *Can. J. For. Res.* **2011**, *41*, 1405–1421. [[CrossRef](#)]
26. Scheller, R.M.; Mladenoff, D.J. An ecological classification of forest landscape simulation models: Tools and strategies for understanding broad-scale forested ecosystems. *Landsc. Ecol.* **2007**, *22*, 491–505. [[CrossRef](#)]
27. Shifley, S.R.; Thompson, F.R.; Dijak, W.D.; Fan, Z.F. Forecasting landscape-scale, cumulative effects of forest management on vegetation and wildlife habitat: A case study of issues, limitations, and opportunities. *For. Ecol. Manag.* **2008**, *254*, 474–483. [[CrossRef](#)]
28. Chang, Y.; He, H.S.; Hu, Y.; Bu, R.; Li, X. Historic and current fire regimes in the Great Xing'an Mountains, northeastern China: Implications for long-term forest management. *For. Ecol. Manag.* **2008**, *254*, 445–453. [[CrossRef](#)]
29. Xu, H.C. *Forest in Great Xing'an Mountains of China*; Science Press: Beijing, China, 1998.
30. Johnstone, J.F.; Chapin, F.S.; Hollingsworth, T.N.; Mack, M.C.; Romanovsky, V.; Turetsky, M. Fire, climate change, and forest resilience in interior Alaska. *Can. J. For. Res.* **2010**, *40*, 1302–1312. [[CrossRef](#)]
31. Van Mantgem, P.J.; Stephenson, N.L.; Byrne, J.C.; Daniels, L.D.; Franklin, J.F.; Fule, P.Z.; Harmon, M.E.; Larson, A.J.; Smith, J.M.; Taylor, A.H.; et al. Widespread increase of tree mortality rates in the western United States. *Science* **2009**, *323*, 521–524. [[CrossRef](#)] [[PubMed](#)]
32. Wang, W.J.; He, H.S.; Spetich, M.A.; Shifley, S.R.; Thompson, F.R.; Larsen, D.R.; Fraser, J.S.; Yang, J. A large-scale forest landscape model incorporating multi-scale processes and utilizing forest inventory data. *Ecosphere* **2013**, *4*, 1–22. [[CrossRef](#)]
33. Parker, G.G.; Harmon, M.E.; Lefsky, M.A.; Chen, J.; Pelt, R.P.; Weiss, S.B.; Thomas, S.C.; Winner, W.E.; Shaw, D.C.; Franklin, J.F. Three-dimensional structure of an old-growth *Pseudotsuga-tsuga* canopy and its implications for radiation balance, and gas exchange. *Ecosystems* **2004**, *7*, 440–453. [[CrossRef](#)]
34. Kane, V.R.; Gersonde, R.F.; Lutz, J.A.; McGaughey, R.J.; Bakker, J.D.; Franklin, J.F. Patch dynamics and the development of structural and spatial heterogeneity in Pacific Northwest forests. *Can. J. For. Res.* **2011**, *41*, 2276–2291. [[CrossRef](#)]
35. Flato, G.M.; Boer, G.J. Warming asymmetry in climate change simulations. *Geophys. Res. Lett.* **2001**, *28*, 195–198. [[CrossRef](#)]
36. Li, X.; He, H.S.; Wu, Z.; Liang, Y.; Schneiderman, J.E. Comparing effects of climate warming, fire, and timber harvesting on a boreal forest landscape in northeastern China. *PLoS ONE* **2013**, *8*, e59747. [[CrossRef](#)] [[PubMed](#)]

37. Yang, J.; He, H.S.; Gustafson, E.J. A hierarchical fire frequency model to simulate temporal patterns of fire regimes in LANDIS. *Ecol. Model.* **2004**, *180*, 119–133. [[CrossRef](#)]
38. Fraser, J.S.; He, H.S.; Shifley, S.R.; Wang, W.J.; Thompson, F.R. Simulating stand-level harvest prescriptions across landscapes: LANDIS PRO harvest module design. *Can. J. For. Res.* **2013**, *43*, 972–978. [[CrossRef](#)]
39. Luo, X.; He, H.S.; Liang, Y.; Wang, W.J.; Wu, Z.W.; Fraser, J.B. Spatial simulation of the effect of fire and harvest on aboveground tree biomass in boreal forests of Northeast China. *Landsc. Ecol.* **2014**, *29*, 1187–1200. [[CrossRef](#)]
40. Liu, Z.; He, H.S.; Yang, J. Emulating natural fire effects using harvesting in an eastern boreal forest landscape of northeast China. *J. Vege. Sci.* **2012**, *23*, 782–795. [[CrossRef](#)]
41. He, H.S.; Mladenoff, D.J.; Crow, T.R. Linking an ecosystem model and a landscape model to study forest species response to climate warming. *Ecol. Model.* **1999**, *114*, 213–233. [[CrossRef](#)]
42. Wang, W.; Peng, C.; Kneeshaw, D.D.; Larocque, G.R.; Song, X.; Zhou, X. Quantifying the effects of climate change and harvesting on carbon dynamics of boreal aspen and jack pine forests using the TRIPLEX-Management model. *For. Ecol. Manag.* **2012**, *281*, 152–162. [[CrossRef](#)]
43. Bodin, P.; Wiman Bo, L.B. The usefulness of stability concepts in forest management when coping with increasing climate uncertainties. *For. Ecol. Manag.* **2007**, *242*, 541–552. [[CrossRef](#)]
44. Perz, S.G.; Muñoz-Carpena, R.; Kiker, G.; Holt, R.D. Evaluating ecological resilience with global sensitivity and uncertainty analysis. *Ecol. Model.* **2013**, *263*, 174–186. [[CrossRef](#)]
45. Carpenter, S.R.; Westley, F.; Turner, M.G. Surrogates for resilience of social-ecological systems. *Ecosystems* **2005**, *8*, 941–944. [[CrossRef](#)]
46. Folke, C.; Carpenter, S.; Walker, B.; Scheffer, M.; Elmqvist, T.; Gunderson, L.; Holling, C.S. Regime shifts, resilience, and biodiversity in ecosystem management. *Annu. Rev. Ecol. Evol. Syst.* **2004**, *35*, 557–581. [[CrossRef](#)]
47. Petchey, O.L.; Gaston, K.J. Effects on ecosystem resilience of biodiversity, extinctions, and the structure of regional species pools. *Theor. Ecol.* **2009**, *2*, 177–187. [[CrossRef](#)]
48. Wang, X.P.; Fang, J.Y.; Zhu, B. Forest biomass and root-shoot allocation in northeast China. *For. Ecol. Manag.* **2008**, *255*, 4007–4020. [[CrossRef](#)]
49. Zhao, M.; Zhou, G.S. Estimation of biomass and net primary productivity of major planted forests in China based on forest inventory data. *For. Ecol. Manag.* **2005**, *207*, 295–313. [[CrossRef](#)]
50. Ivanova, G.A.; Conard, S.G.; Kukavskaya, E.A.; McRae, D.J. Fire impact on carbon storage in light conifer forests of the Lower Angara region, Siberia. *Environ. Res. Lett.* **2011**, *6*, 045203. [[CrossRef](#)]
51. Wang, W.J.; He, H.S.; Spetich, M.A.; Shifley, S.R.; Thompson, F.R.; Dijak, W.D.; Wang, Q. A framework for evaluating forest landscape model predictions using empirical data and knowledge. *Environ. Model. Softw.* **2014**, *62*, 230–239. [[CrossRef](#)]
52. Wang, X.C.; Zhang, Y.D.; McRae, D.J. Spatial and age-dependent tree-ring growth responses of *Larix gmelinii* to climate in northeastern China. *Trees Struct. Funct.* **2009**, *23*, 875–885. [[CrossRef](#)]
53. Luo, X.; Wang, Y.; Zhang, J. Simulating the effects of climate change and fire disturbance on aboveground biomass of boreal forests in the Great Xing'an Mountains, Northeast China. *Chin. J. Appl. Ecol.* **2018**, *29*, 713–724.
54. Leng, W.; He, H.S.; Bu, R.; Dai, L.; Hu, Y.; Wang, X. Predicting the distributions of suitable habitat for three larch species under climate warming in Northeastern China. *For. Ecol. Manag.* **2008**, *254*, 420–428. [[CrossRef](#)]
55. Lenoir, J.; Gégout, J.C.; Marquet, P.A.; Ruffray, P.D.; Brisse, H. A significant upward shift in plant species optimum elevation during the 20th century. *Science* **2008**, *320*, 1768–1771. [[CrossRef](#)] [[PubMed](#)]

